I S A V

Journal of Theoretical and Applied Vibration and Acoustics

journal homepage: http://tava.isav.ir

Experimental investigation of the gyroscopic and rotary inertia effects on the chatter boundary in a milling process

Ali Mokhtari [a], **Mohammad Mahdi Jalili** [b], **Abbas Mazidi** [*c]

[a] *PhD Candidate, Department of Mechanical Engineering, Yazd University, yazd, Iran*

[b] *Associate Professor, Department of Mechanical Engineering, Yazd University, yazd, Iran*

[c] *Assistant Professor, Department of Mechanical Engineering, Yazd University, yazd, Iran*

ARTICLE INFO

Article history:
Received 2 November 2018

Received in revised form
5 June 2019

Accepted 10 December 2019

Available online 23 December 2019

Keywords:
Experimental investigation,

Rotary inertia and gyroscopic moments,

Chatter,

Milling,

Timoshenko beam theory,

Stability lobe diagram.

ABSTRACT

Experimental examination of the gyroscopic and rotary inertia effects on the chatter boundary in a milling operation is the chief aim of this article. The equations of motion of the tool vibration are derived based on Timoshenko beam theory and Hamilton principle by considering gyroscopic moment, rotary inertia, velocity-dependent process damping and radial immersion effect. For a range of depth of cuts and spindle velocities, the stability of the milling process is determined by using the method of multiple scales and creating a so-called stability lobe diagram (SLD) in which boundaries separate stable area and unstable or chatter area. Then the newly obtained SLD with the effects of rotary inertia and gyroscopic moments is verified experimentally. Indeed, the verification of the lobes at the speeds where the distinction is sound between the conventional lobes and the newly obtained lobes is presented. Here, the SLD obtained without the effects of rotary inertia and gyroscopic moments is so-called conventional SLD. For this purpose, some experiments are conducted to demonstrate the progressive move into the unstable zone at the locally optimum point of SLD. Finally, a parametric study is presented as a validation of the newly obtained lobes from the sense that the effects of different parameters on these limits are as expected.

1. Introduction

One essential concern in cutting operations is the so-called regenerative chatter that is the most frequent type of self-excited vibration between the machine tool and the work-piece. Milling is one of the most frequently used operations for machining a wide variety of work-pieces to

[*] Corresponding author:
E-mail address: amazidi@yazd.ac.ir (A. Mazidi)

http://dx.doi.org/10.22064/tava.2020.96841.1120

generate high-accurate parts and first-rate surface finish. This vibration, from a technical point of view, is the basic obstruction to guarantee precision and productivity in the machining industry. The incidence of chatter may damage the cutter and scrap the work-piece.

A review of the literature on the subject of the chatter problem confirms that the existing studies can be divided into two classifications. The first class includes all those researches that used finite degrees of freedom (DoF) in a dynamic model to study machining processes. The second class encompasses all those studies that focused on the continuous systems for machining process.

In terms of the first classification, the models used in these studies are mostly 2-dimensional (2-D) space and Multi-DoF with many simplifying assumptions. One of the first studies, which were conducted to identify the regenerative effect as the most important cause of chatter, is due to Hanna and Tobias [1]. Lin and Weng [2] represented a set of coupled second-order differential equations for a 2-DoF dynamic model of the cutting process by considering nonlinear stiffness and nonlinear time-delay terms. Altintas and Budak [3] developed an analytical approach based on transfer functions for constructing SLD of a 2-DoF model of the milling operation. Nayfeh *et al*. [4] used the model of Ref. [1] and developed the machine tool dynamics from static cutting to chaos using a variety of analytical and computational tools. Altintas and Budak [5] extended the model of Ref. [3] by adding the compliance-damping terms in two directions due to the behavior of the work-piece. Balachandran and zhao[6] studied work-piece/tool interactions during milling of ductile work-pieces with helical tools with a multi-DoF unified mechanics-based model. Pratt and Nayfeh [7] studied the chatter stability improvement of machining processes by the addition of tuned active vibration absorbers to the structure. Deshpande and Fofana[8] examined the chaotic behavior of chatter by considering nonlinear damping and stiffness terms. Moon and Kalmar-Nagy [9] illustrated that single-DoF models are not suitable for studying behavior of cutter chaos and models with more complexity, such as multi-DoFs based on careful cutting force experiments, are required. Balachandran [10] showed that more than one time delay parameters are required to study the stability of a general milling process. Fofana [11] investigated the stability behavior of machine chatter with deterministic and stochastic perturbations by using the delay dynamical system theories. Mann *et al*. [12] scrutinized the influences of asymmetric structural modes and the effects of nonlinear regeneration in a discontinuous cutting force with a 2-DoF model. Budak and Ozlu [13] developed a systematic model for constructing SLD in boring and turning processes. In addition, they [14] built up a comparative examination between 1-D and poly-dimensional steadiness representations for turning operations. Vela-Martínez *et al*. [15]presented a single DoF nonlinear model of a machining process and used the method of multiple scales (MMS) to analyze the self-generated vibrations of that process. Moradi *et al*. [16] illustrated a nonlinear 2-DoF model to study chatter vibrations analytically in milling operation via the MMS. Besides, they [17] examined tool wear and process damping effects in their model. Li *et al*.[18] presented 1- and 2-DoF models of milling processes and used the complete discretization approach, which has more accuracy and reliability than semi- and full-discretization methods, to study those processes. Jin *et al*.[19] proposed an improved calculation to forecast the SLD of 2-DoF milling operation with a changeable pitch cutter.

Contrary to the first classification, the second one included fewer efforts. Liao and Tsai[20] applied the finite element method (FEM) on a pre-twisted Timoshenko beam model of the helical

fluted cutting tool to calculate dynamic tool displacements and cutting forces. Salahshoor and Ahmadian[21] modeled the cutter and cutter-holder joints with an Euler Bernoulli beam element and torsional/translational dampers/springs, respectively, to obtain the SLD. Catania and Mancinelli [22] suggested a discrete modal procedure in terms of Euler Bernoulli beam mode shapes for the cutting tool. Movahhedy and Mosaddegh [23] studied the stability of a high-speed milling structure with Timoshenko beam model based on finite element matrices in the presence of gyroscopic effects. Tajalli *et al*.[24, 25] examined the stability of a micro end-mill tool by applying a numerical method on formulations of the structure that were obtained from strain gradient and Timoshenko beam theories. Tavari *et al*. [26] modeled the work-piece in turning operations as a 3-D nonlinear spinning cantilever Euler Bernoulli beam. They used a combination of mode-summation and Runge-Kutta methods to achieve an approximated solution of their model and scrutinize the effect of some features on the stability results. Jalili and Emami [27] applied the MMS on the previous work formulations to derive an analytical solution. Jalili *et al*.[28] studied several types of resonances by using a 3-D spinning cantilever Rayleigh beam model for the milling tool by considering structural nonlinearities and gyroscopic and rotary inertial dynamics. Mokhtari *et al*. [29] modeled the milling tool as a 3-D linear spinning cantilever bending-bending-torsion Timoshenko beam by considering gyroscopic and rotary inertial dynamics. They used an analytical-numerical method, so-called spectral finite element scheme, to construct the SLD. Mokhtari *et al*. [30] scrutinized the chatter phenomenon by using a 3-D elastic nonlinear dynamic model of the micro-milling tool with including structural nonlinearities, gyroscopic moment, rotary inertia, process damping and size effect. They verified their analytical effort by comparing simulated results with the results obtained from chatter tests and literature.

Based on the literature review, the major contribution of current work is the experimental verification of formerly published theoretical works[30]. In other words, the verification of the lobes at the speeds where the distinction is sound between the conventional lobes and the newly-obtained lobes is the main purpose of the presented study.

2. Equations of motion

Fig. 1 shows a 3-D spinning clamped-free Timoshenko beam that is considered to model the milling tool. The geometrical uniformity assumption of the milling tool is included in this model. In reference to Fig. 1, the axes XYZ and corresponding unit bases vectors $\boldsymbol{IJK}$ organized a fixed inertial coordinate system $\mathfrak{R}$, and axes xyz and corresponding unit bases vectors $\boldsymbol{ijk}$ formed a local coordinate system $\mathfrak{V}$ attached to the centerline of the spindle. Spindle framework $\mathfrak{V}$ tracks the rigid body movement of the milling tool that means this framework rotates with respect to $\mathfrak{R}$ at a constant spindle speed $\Omega \boldsymbol{i}$.

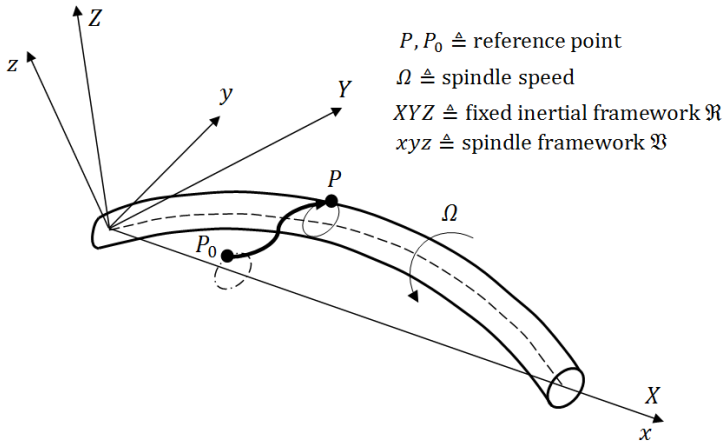

Fig. 1. Schematic of a deformed milling tool in fixed framework $\mathfrak{R}$ and spindle framework $\mathfrak{V}$.

The order three equations of motion for the nonlinear Timoshenko beam model of the milling tool can be obtained as explained in Ref. [30] by considering classical continuum beam theory.

3. Non-dimensional equations of motions

Typically, the dimensionless methodology generalizes the problem. From the viewpoint of the milling process, the analysis of dimensional form is the analysis of a particular problem. Unlike this, non-dimensional analysis can be established by a set of dimensionless parameters. Using a non-dimensional analysis can illustrate various dimensional solutions. The dimensionless factors utilized for current research are tabulated in Table 1.

Table 1. Non-dimensional parameters

Symbol	Definition	Symbol	Definition
(x^*, d_t^*, a^*, s_f^*)	$(x, d_t, a, s_f)/L$	ω_n^*	ω_n/ϖ
L^*	L/L	$\mathfrak{C}_B^*$	$\{\mathfrak{C}_B/\rho\varpi L^2\} = 2\zeta_B\omega_n^* A^*$
ρ^*	ρ/ρ	$\mathfrak{C}_R^*$	$\{\mathfrak{C}_R/\rho\varpi L^4\} = 2\zeta_R\omega_n^* I^*$
t^*	ϖt	(w_y^*, w_z^*)	$(w_y, w_z)/L$
ϖ	$\sqrt{EI/\rho AL^4}$	(ϕ_y^*, ϕ_z^*)	(ϕ_y, ϕ_z)
A^*	A/L^2	(G^*, E^*, K_t^*, K_r^*)	$(G, E, K_t, K_r)/\rho\varpi^2 L^2$
I^*	I/L^4	(G_t^*, G_r^*)	$(G_t, G_r)/\rho\varpi^2 L^3$
Ω^*	Ω/ϖ	δ_D^*	$L\delta_D$

In Table 1, the parameters w_y and w_z are the lateral deflections at the spindle frame, respectively. Besides, $\phi_z(x,t)$ and $\phi_y(x,t)$ are rotations due to w_y and w_z, respectively. In addition, parameters $\{K_t, K_r\}$ are the cutting factors of movements in tangential and radial directions, parameters $\{G_r, G_t\}$ are the process damping coefficients in radial and tangential

direction, a is the depth of the cut, d_t is the tool diameter, and $\mathcal{s}_f$ is the feed per tooth. Besides, parameters ω_n, ζ_B, ζ_R, ρ, A, L, E, and G represent the mass per unit volume, the natural frequency, the damping ratio in the bending movement, the damping ratio in the rotary movement, the cross-section area, the length of the tool, Young's modulus, and the shear modulus, respectively. The symbols $\mathfrak{C}_B$ and $\mathfrak{C}_R$ indicate damping coefficients in the bending and rotary movements, respectively.

4. Reduced-order model

For solving the milling tool's non-dimensional PDEs, the Galerkin method is employed to reduce the equations to dimensionless ODEs. Consequently, the functions w_y^*, w_z^*, ϕ_y^*, and ϕ_z^* can be presented as the multiplication of two separated non-dimensional spatial and time functions as:

$$w_y^*(x^*,t^*) = \mathcal{W}_y(x^*)T_{w_y}(t^*), \qquad w_z^*(x^*,t^*) = \mathcal{W}_z(x^*)T_{w_z}(t^*) \tag{1}$$

$$\phi_z^*(x^*,t^*) = \Xi_z(x^*)T_{\phi_z}(t^*), \qquad \phi_y^*(x^*,t^*) = \Xi_y(x^*)T_{\phi_y}(t^*) \tag{2}$$

where $\mathcal{W}_y = \mathcal{W}_z = Y$ and $\Xi_z = -\Xi_y = \Theta$ are the fundamental non-dimensional mode shapes of a non-rotating milling tool in bending and transverse rotation obtained from the dynamic stiffness matrix scheme [24, 28], respectively. Now with multiplying non-dimensional mode shape functions on each side of PDEs of motion and integrating over the tool non-dimensional length, the acquired ODEs can be obtained:

$$\begin{aligned}
&\text{Ⱥ}_1T_{w_y,tt} + \text{Ⱥ}_2T_{w_z,t} + \text{Ⱥ}_3T_{w_y} + \text{Ⱥ}_4T_{\phi_z} + \text{Ⱥ}_5T_{w_y}^3 + \text{Ⱥ}_6T_{w_y}T_{w_z}^2 + \text{Ⱥ}_7T_{w_y}T_{\phi_z}^2 + \text{Ⱥ}_8T_{w_y}T_{\phi_y}^2 + \text{Ⱥ}_9T_{\phi_z}^3 \\
&\quad + \text{Ⱥ}_{10}T_{\phi_z}T_{\phi_y}^2 + \text{Ⱥ}_{11}T_{w_z}T_{\phi_z}T_{\phi_y} + \text{Ⱥ}_{12}T_{w_y,t} = \mathcal{F}_{w_y}, \\
&\text{Ɓ}_1T_{\phi_z,tt} + \text{Ɓ}_2T_{\phi_z} + \text{Ɓ}_3T_{w_y} + \text{Ɓ}_4T_{\phi_z}^3 + \text{Ɓ}_5T_{\phi_z}T_{\phi_y}^2 + \text{Ɓ}_6T_{\phi_z}T_{w_y}^2 + \text{Ɓ}_7T_{\phi_z}T_{w_z}^2 + \text{Ɓ}_8T_{w_y}T_{\phi_z}^2 + \text{Ɓ}_9T_{w_y}T_{\phi_y}^2 \\
&\quad + \text{Ɓ}_{10}T_{\phi_z,tt}T_{\phi_y}^2 + \text{Ɓ}_{11}T_{\phi_y,t}T_{\phi_y}^2 + \text{Ɓ}_{12}T_{w_y}T_{w_z}T_{\phi_y} + \text{Ɓ}_{13}T_{w_z}T_{\phi_z}T_{\phi_y} \\
&\quad + \text{Ɓ}_{14}T_{\phi_z,t}T_{\phi_y,t}T_{\phi_y} + \text{Ɓ}_{15}T_{\phi_z,t} = 0, \\
&\text{€}_1T_{w_z,tt} + \text{€}_2T_{w_y,t} + \text{€}_3T_{w_z} + \text{€}_4T_{\phi_y} + \text{€}_5T_{w_z}^3 + \text{€}_6T_{w_z}T_{w_y}^2 + \text{€}_7T_{w_z}T_{\phi_y}^2 + \text{€}_8T_{w_z}T_{\phi_z}^2 + \text{€}_9T_{\phi_y}^3 \\
&\quad + \text{€}_{10}T_{\phi_y}T_{\phi_z}^2 + \text{€}_{11}T_{w_y}T_{\phi_y}T_{\phi_z} + \text{€}_{12}T_{w_z,t} = \mathcal{F}_{w_z}, \\
&\text{£}_1T_{\phi_y,tt} + \text{£}_2T_{\phi_y} + \text{£}_3T_{w_z} + \text{£}_4T_{\phi_y}^3 + \text{£}_5T_{\phi_y}T_{\phi_z}^2 + \text{£}_6T_{\phi_y}T_{w_y}^2 + \text{£}_7T_{\phi_y}T_{w_z}^2 + \text{£}_8T_{w_z}T_{\phi_y}^2 + \text{£}_9T_{w_z}T_{\phi_z}^2 \\
&\quad + \text{£}_{10}T_{\phi_y}T_{\phi_{z,t}}^2 + \text{£}_{11}T_{\phi_{z,t}}T_{\phi_y}^2 + \text{£}_{12}T_{w_z}T_{w_y}T_{\phi_z} + \text{£}_{13}T_{\phi_y}T_{\phi_z}T_{w_y} + \text{£}_{14}T_{\phi_{y,t}} = 0.
\end{aligned} \tag{3}$$

where

$$\begin{aligned}
\mathcal{F}_{w_y} &= \text{Ⱥ}_{13}\Delta T_{w_y} + \text{Ⱥ}_{14}\Delta T_{w_z} + \text{Ⱥ}_{15} + \text{Ⱥ}_{16}T_{w_y,t} + \text{Ⱥ}_{17}T_{w_z,t}, \\
\mathcal{F}_{w_z} &= \text{€}_{13}\Delta T_{w_y} + \text{€}_{14}\Delta T_{w_z} + \text{€}_{15} + \text{€}_{16}T_{w_y,t} + \text{€}_{17}T_{w_z,t}.
\end{aligned} \tag{4}$$

in which $\wp_{,\mathscr{b}} \triangleq \partial\wp/\partial\mathscr{b}$, $\Delta\wp = \wp - \wp_\tau$, $\wp_\tau \triangleq \wp(x, t-\tau)$, $\tau = 2\pi/N\Omega$ is delay time, and N is the total number of teeth.

5. Multiple scale method

The method of multiple-scale (MMS) is a strong approach among perturbation methods for solving nonlinear equations. Based on MMS, the proposed solution of Eq. (3) is:

$$\begin{aligned} T_{w_y}(t^*,\varepsilon) &= q(t^*,\varepsilon) = q_0(T_0,T_1) + \varepsilon q_1(T_0,T_1) + O(\varepsilon^2), \\ T_{\phi_z}(t^*,\varepsilon) &= \hbar(t^*,\varepsilon) = \hbar_0(T_0,T_1) + \varepsilon \hbar_1(T_0,T_1) + O(\varepsilon^2), \\ T_{w_z}(t^*,\varepsilon) &= \wp(t^*,\varepsilon) = \wp_0(T_0,T_1) + \varepsilon \wp_1(T_0,T_1) + O(\varepsilon^2), \\ T_{\phi_y}(t^*,\varepsilon) &= \mathcal{r}(t^*,\varepsilon) = \mathcal{r}_0(T_0,T_1) + \varepsilon \mathcal{r}_1(T_0,T_1) + O(\varepsilon^2). \end{aligned} \tag{5}$$

The character ε is a small factor representing the time scale [31]. In order to have the nonlinear, time delay, viscous and process damping terms appear in the same perturbation equations, some coefficients should be scaled as follows:

$$\begin{aligned} \text{Ⱥ}_i &= \varepsilon \text{Ⱥ}_i^{"}, & i &= 5,6,7,\dots,17. \\ \text{Ɓ}_j &= \varepsilon \text{Ɓ}_j^{"}, & j &= 4,5,6,\dots,15. \\ €_m &= \varepsilon €_m^{"}, & m &= 5,6,7,\dots,17 \\ £_n &= \varepsilon £_n^{"}, & n &= 4,5,6,\dots,14. \end{aligned} \tag{6}$$

Applying MMS and substituting Eqs. (5) and (6) into Eq. (3) and arranging based on ε^0 and ε^1, the solution of the zero-order equation can be supposed as follows:

$$\begin{aligned} q_0 &= \sum_{r=1}^{4} \mathbb{Q}_{0r}(T_1)\exp(i\omega_r T_0) + cc, & \hbar_0 &= \sum_{r=1}^{4} \Lambda_{1r}\mathbb{Q}_{0r}(T_1)\exp(i\omega_r T_0) + cc, \\ \wp_0 &= \sum_{r=1}^{4} \Lambda_{2r}\mathbb{Q}_{0r}(T_1)\exp(i\omega_r T_0) + cc & \mathcal{r}_0 &= \sum_{r=1}^{4} \Lambda_{3r}\mathbb{Q}_{0r}(T_1)\exp(i\omega_r T_0) + cc, \end{aligned} \tag{7}$$

$$\begin{aligned} &(\gamma_{1\Re} + i\gamma_{1\Im})\text{א}_1 + (i\gamma_{2\Im})\text{א}_1\text{א}_2^2 + (i\gamma_{3\Im})\text{א}_1\text{א}_3^2 + (i\gamma_{4\Im})\text{א}_1\text{א}_4^2 + (i\gamma_{5\Im})\text{א}_1^3 + (\gamma_{6\Re})\dot{\text{א}}_1 \\ &\quad + (i\gamma_{7\Im})\text{א}_1\dot{\text{ב}}_1 = 0, \\ &(\lambda_{1\Re} + i\lambda_{1\Im})\text{א}_2 + (i\lambda_{2\Im})\text{א}_2\text{א}_1^2 + (i\lambda_{3\Im})\text{א}_2\text{א}_3^2 + (i\lambda_{4\Im})\text{א}_2\text{א}_4^2 + (i\lambda_{5\Im})\text{א}_2^3 + (\lambda_{6\Re})\dot{\text{א}}_2 \\ &\quad + (i\lambda_{7\Im})\text{א}_2\dot{\text{ב}}_2 = 0, \\ &(\mu_{1\Re} + i\mu_{1\Im})\text{א}_3 + (i\mu_{2\Im})\text{א}_3\text{א}_1^2 + (i\mu_{3\Im})\text{א}_3\text{א}_2^2 + (i\mu_{4\Im})\text{א}_3\text{א}_4^2 + (i\mu_{5\Im})\text{א}_3^3 + (\mu_{6\Re})\dot{\text{א}}_3 \\ &\quad + (i\mu_{7\Im})\text{א}_3\dot{\text{ב}}_3 = 0, \\ &(\chi_{1\Re} + i\chi_{1\Im})\text{א}_4 + (i\chi_{2\Im})\text{א}_4\text{א}_1^2 + (i\chi_{3\Im})\text{א}_4\text{א}_2^2 + (i\chi_{4\Im})\text{א}_4\text{א}_3^2 + (i\chi_{5\Im})\text{א}_4^3 + (\chi_{6\Re})\dot{\text{א}}_4 \\ &\quad + (i\chi_{7\Im})\text{א}_4\dot{\text{ב}}_4 = 0. \end{aligned} \tag{8}$$

where cc stands for the complex conjugate of the prior terms. Moreover, the parameters ω_r and $\{\Lambda_{1r}, \Lambda_{2r}, \Lambda_{3r}\}$ are the real positive eigenvalues and corresponding eigenvectors, respectively, that are related to the zero-order equation. Substituting the solution of the zero-order equation into the first-order equation and eliminating the terms that lead to secular terms, solvability condition can be obtained in a non-resonant excitation case. In this case, putting $\mathbb{Q}_{0r} = \text{א}_r(T_1)\exp[i\text{ב}_r(T_1)]$ in the equations resultant from secular terms leads to:

where $\dot{\wp} \triangleq d\wp/dT_1$. Separating real and imaginary parts of Eq. (8) yields the solution of $\aleph_r(T_1)$ and $\beth_r(T_1)$. Based on the solutions, the tool can be experienced chatter phenomena in the following conditions:

$$\frac{\gamma_{1\Re}}{\gamma_{6\Re}} < 0, \qquad \frac{\lambda_{1\Re}}{\lambda_{6\Re}} < 0, \qquad \frac{\mu_{1\Re}}{\mu_{6\Re}} < 0, \qquad \frac{\chi_{1\Re}}{\chi_{6\Re}} < 0. \tag{9}$$

6. Results and discussion

To analyze the stability of the milling process, a set of realistic nominal values of the necessary parameters presented by Moradi *et al*. [32] are listed in Table 2.

Table 2. Necessary parameters introduced by Moradi *et al*. [32]

Parameter	Value	Parameter	Value
Tool material	High-speed steel (HSS)	ζ_B (z − direction)	0.1
Work-piece material	AL7075	a_e/d_t	1
L	78.5 mm	G_r	−
d_t	14 mm	G_t	−
N	4	Stable depth at $\Omega = 8000$ rpm	9.5 mm
K_r	194 N/mm^2	Unstable depth at $\Omega = 8000$ rpm	10.5 mm
K_t	63.5 N/mm^2	Stable depth at $\Omega = 10000$ rpm	11.5 mm
ζ_B (y − direction)	0.098	Unstable depth at $\Omega = 10000$ rpm	12.5 mm

Based on the values of parameters tabulated in Table 2 and Eq. (9), the corresponding SLD can be constructed with and without gyroscopic and rotary effects by the solution method of the current work as Fig. 2. Moreover, the experimental results obtained by Moradi *et al*.[32] are presented in Fig. 2. This figure shows that the results obtained from the current model are in excellent agreement with the experimental results derived by Moradi *et al*.[32]. In all SLDs of the current effort, the area down/up the lobes is stable/unstable zone for milling operation.

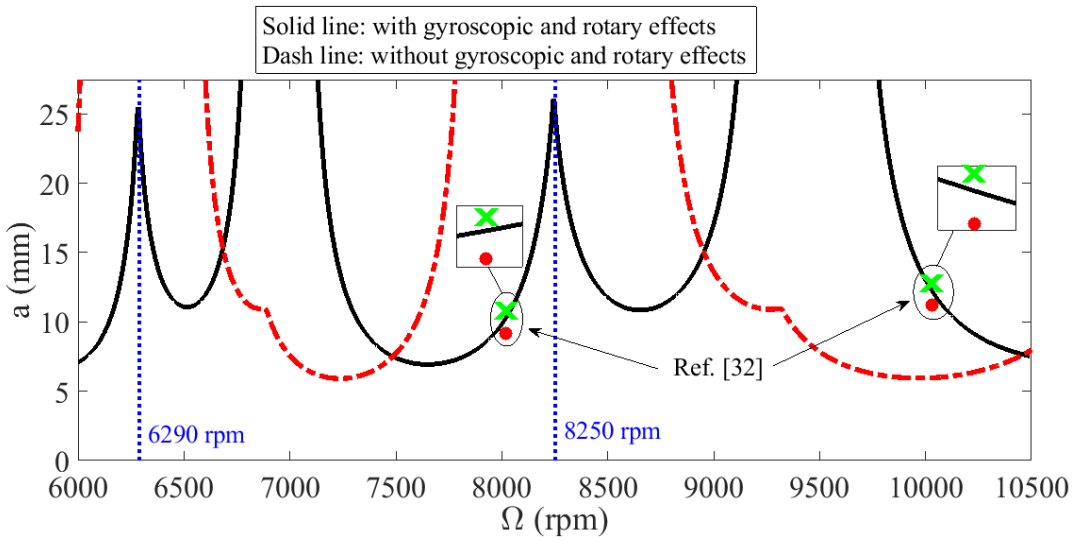

(a)

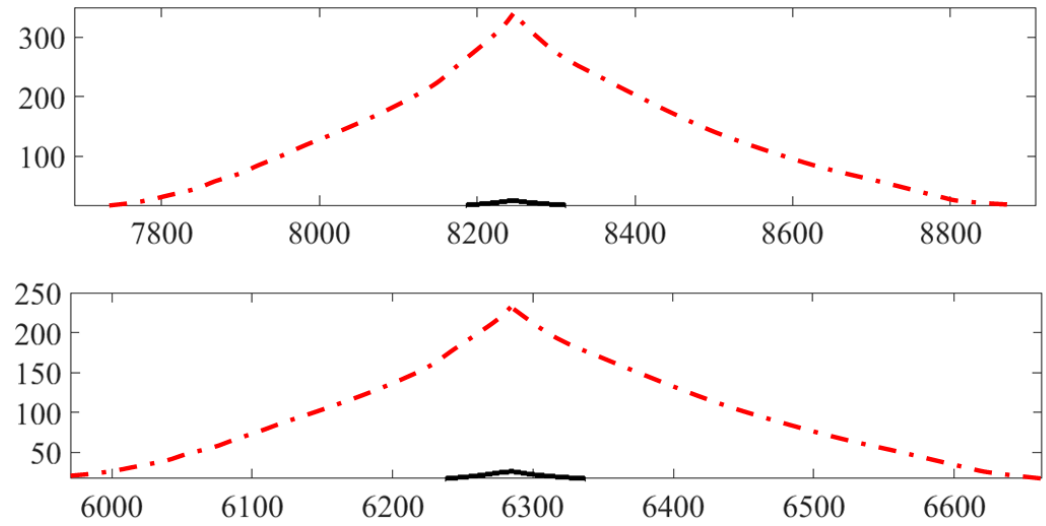

(b)

Fig. 2. Effect of gyroscopic and rotary terms on the stability of the system (solid line: with gyroscopic and rotary effects, dash line: without gyroscopic and rotary effects), (a) Analytical and laboratory-measured stability lobe (the signs × and ● show unstable and stable conditions), and (b) Zoom-in on SLD at speeds 6290 and 8250 rpm.

From Fig. 2, it can be seen that disregarding the effects of rotary inertia and gyroscopic moments in the modeling of the milling tool causes significant errors on the stability estimation, especially on the locally optimum point of SLD. It seems like the speeds of 8000 and 10000 rpm are not where the current model distinguishes itself from a model without gyroscopic and rotary effects such as the model of Ref. [32]. Take into account that Mokhtari *et al*. [30] have formerly published the solution method of the current study. However, it is interesting to validate this solution method at speeds where the distinction is sound (say at 6290 and 8250 rpm). Therefore,

the main purpose of this section is an experimental investigation of the gyroscopic and rotary inertia effects on the chatter boundary in the presented milling process.

For this purpose, a number of chatter tests are performed on an in-house CNC machine with maximum spindle speed $\Omega = 10000$ rpm. It should be noted that the milling tool and work-piece are selected as introduced in Table 2. The experimental setup is shown in Fig. 3.

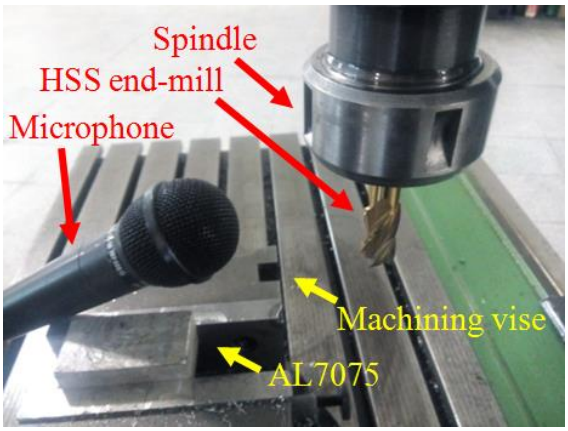

Fig. 3. The chatter test setup.

Generally, the chatter frequency is a frequency near the tool natural frequency. Therefore, it is essential to find the natural frequency of the tool. The natural frequency of the cutting tool is extracted using a modal test based on Fig. 4.

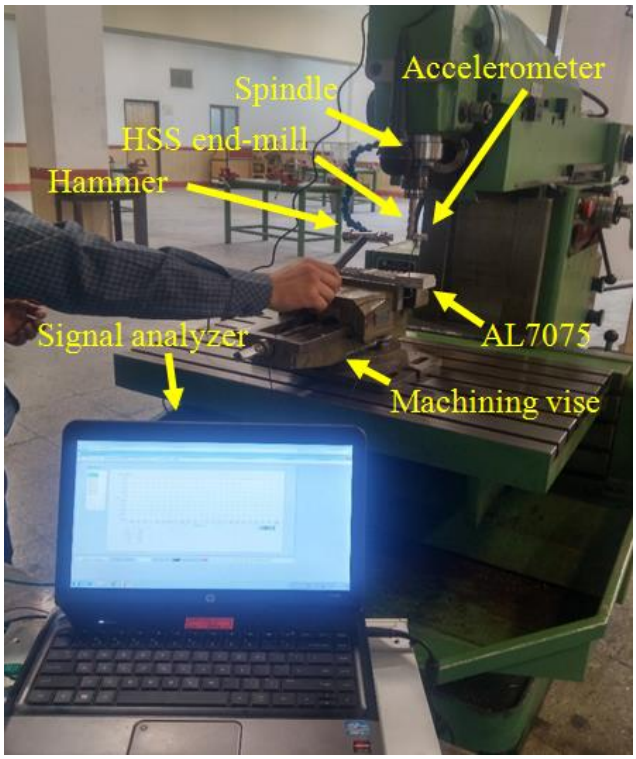

Fig. 4. The modal test setup of the tool-tip in the lateral direction.

For modal tests, a signal analyzer type VibroRack 1000 made by ABP corporation is used. A piezo-electric type accelerometer type AP203-100 made by Global Test for response measurement and the hammer type AU-02 made by Global Test is used for the modal test. The modal tests are carried out in the lateral direction. The modal tests are repeated five times and frequency response is achieved by averaging of these data. The frequency response of receptance function, between the exerted force and tool displacement in the lateral direction is presented in Fig. 5.

The first tool natural frequency from the modal test is close to 1600 Hz and from the dynamic stiffness matrix method (see section 4 of Ref. [30] and section 3.2 of Ref.[24]) is 1618.63 Hz. Comparing these values shows the accuracy of the proposed model.

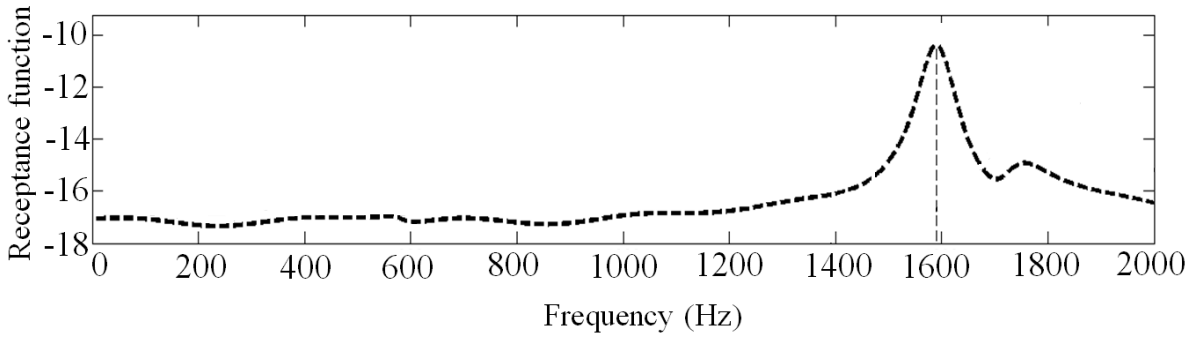

Fig. 5. The frequency response of the receptance function of the tool tip in the lateral direction.

To detect chatter frequency, a microphone is used to measure the sound signals during cutting tests (see Fig. 3). Each chatter test at a certain spindle speed and a certain cutting depth is executed six times. Corresponding fast Fourier transform (FFT) of the resultant sound signals at spindle speeds $\Omega = 6290{,}8250$ rpm are presented in Fig. 6(a) and Fig. 6(b), respectively. In these figures, the FFT diagrams of all experiments at a certain spindle speed are compressed into a 3D plot. These experiments are conducted to demonstrate the progressive move into the unstable zone. Chatter is recognized when the magnitude of sound spectrums at a frequency near the tool natural frequency becomes relatively high. In addition, the other peaks are at the tooth passing frequency harmonics. Consequently, based on Fig. 6(a) and Fig. 6(b), the peak appeared at 1600 Hz is due to chatter occurrence and the other peaks are related to the tooth passing frequency harmonics. As a result, the tool at $\Omega = 6290{,}8250$ rpm and depth of cut $a = 24.0{,}25.0 \pm 0.4$ mm is stable, respectively. Also, chatter can happen at $\Omega = 6290, 8250$ rpm and depth of cut $a = 25.5{,}26.5 \pm 0.4$ mm, respectively. It should be noted that 419.3 and 550 Hz are the tooth passing frequency at $\Omega = 6290$ and 8250 rpm, respectively. These experimental results and constructed SLD with/without gyroscopic and rotary inertia effects are presented in Fig. 6(c).

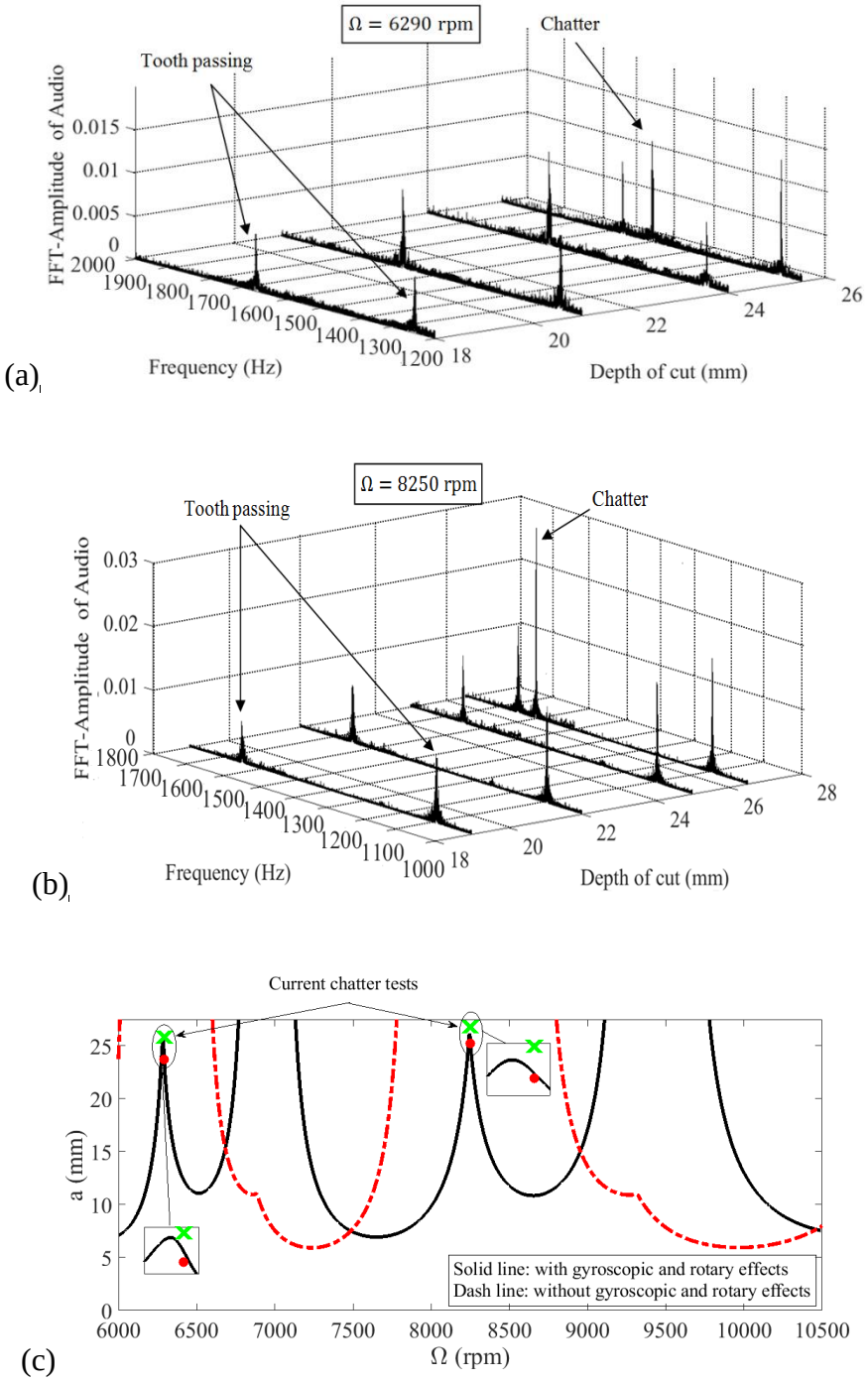

Fig. 6. (a) The FFT diagrams of sound signals at $\Omega = 6290$ rpm, (b) The FFT diagrams of sound signals at $\Omega = 8250$ rpm, (c) Analytical and laboratory-measured stability lobe (signs × and ● show unstable and stable conditions).

Surface conditions for these spindle speeds are also shown in Fig. 7. As shown in Fig. 7(a) and Fig. 7(b), at spindle speed $\Omega = 6290,8250$ rpm for the depth of cut bellow $a = 25.5,26.5$ mm, respectively, the machined surface has a smooth finish without ripples. But at the depth of cut

$a = 25.5,26.5$ mm, respectively, the machined surface exhibits an undulated finish. These results confirm the results obtained from the sound test.

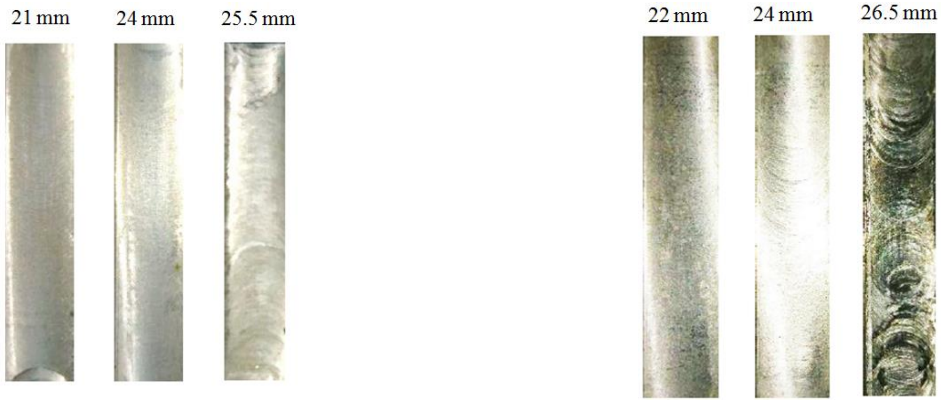

(a) (b)

Fig. 7. Surface finish results at different cutting depths at spindle speeds (a) $\Omega = 6290$ rpm, (b) $\Omega = 8250$ rpm.

Therefore, the SLD obtained with the effects of rotary inertia and gyroscopic moments is verified experimentally at the speeds where the distinction is sound between the conventional lobes and the newly obtained lobes in Fig. 6 and Fig. 7. In other words, Fig. 6 and Fig. 7 depict the experimental inspection of the gyroscopic and rotary inertia effects on the chatter stability in the current milling process.

Here, a parametric study is presented. Fig. 8 explains the effects of force coefficients on the chatter occurrence probability. These figures demonstrate that decreasing the tangential and radial force coefficients may lead to increase the stability and vice versa. Some realistic examples of reducing these coefficients are submerging the tool/work-piece system in viscous fluid[33] and using cryogenic cooling system during milling process [34]:

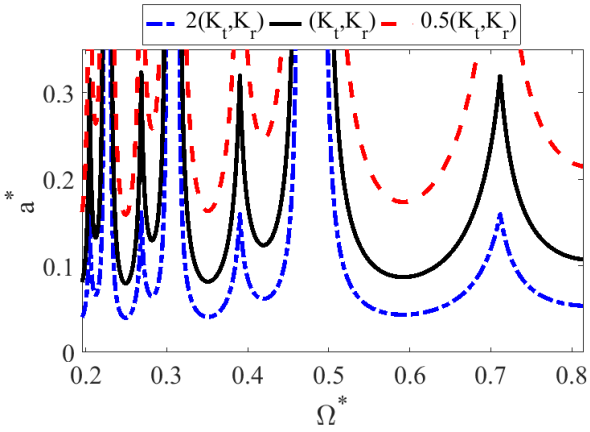

(c)

Fig. 8. Effect of generative force coefficients on the stability of the system.

The effect of immersion ratio on the stability area of the tool is showed up in Fig. 9. The most notable viewpoint of this figure is that the smaller immersion ratio estimates more stability than does the bigger one.

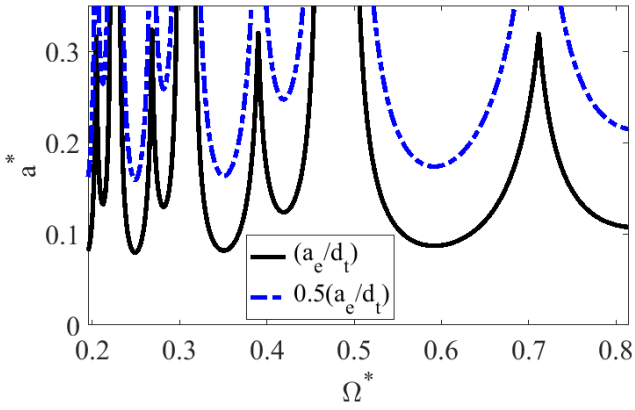

Fig. 9. Effect of immersion ratio on the stability of the system.

The effect of the tool length on the chatter stability is illustrated in Fig. 10. Because the dimensionless parameters corresponding to spindle speed and cutting depth change by varying the tool length, Fig. 10 is presented with dimensional parameters. It can be seen from the mentioned figure that increasing tool length can stretch the lobes, reduce the number of lobes, and decrease the stability of the process.

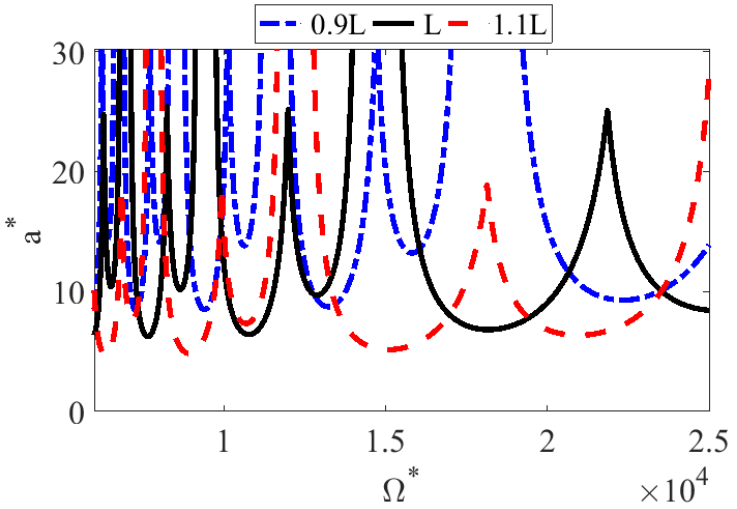

Fig. 10. Effect of tool length on the stability of the system.

The influence of the tool diameter on SLD of the operation is presented in Fig. 11. For the reason that the non-dimensional parameter related to spindle speed changes by varying the tool diameter, Fig. 11 is conducted based on dimensional parameters. According to the mentioned figure, the SLD achieves a horizontal and vertical shift by varying tool diameter. Generally, increasing this parameter can enlarge the stability of the process.

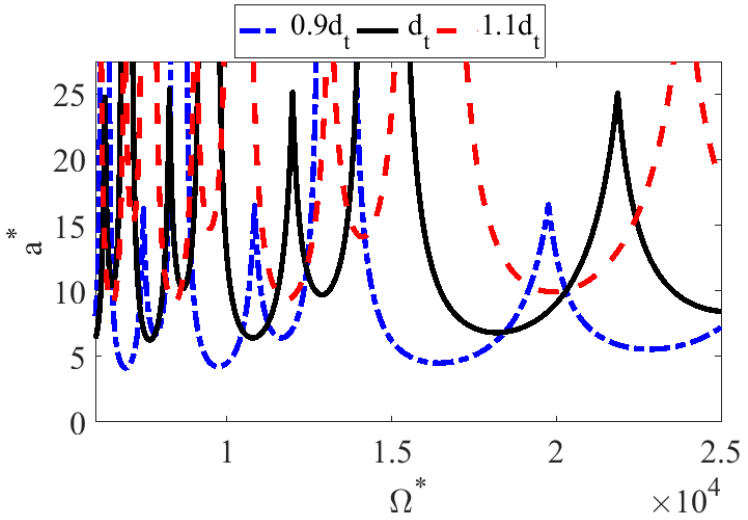

Fig. 11. Effect of tool diameter on the stability of the system.

The parametric study is presented as a validation of the newly-obtained lobes from the sense that the effects of different parameters on these limits are as expected.

7. Conclusion

In this research, the prediction of chatter occurrence in the milling operation has been examined by employing a 3-D nonlinear dynamic model of the milling tool. A spinning cantilever Timoshenko beam that is excited by the cutting forces is used to model the cutting tool. The multiple scales method has been used to achieve analytical responses for nonlinear delay partial differential equations of motion. The obtained SLD with the effects of rotary inertia and gyroscopic moments has been validated experimentally. Indeed, the validation of the lobes at the speeds where the distinction is sound between the conventional lobes and the newly obtained lobes has been illustrated.

References

[1] N.H. Hanna, S.A. Tobias, A theory of nonlinear regenerative chatter, (1974).
[2] J.S. Lin, C.I. Weng, Nonlinear dynamics of the cutting process, International Journal of Mechanical Sciences, 33 (1991) 645-657.
[3] Y. Altintaş, E. Budak, Analytical prediction of stability lobes in milling, CIRP annals, 44 (1995) 357-362.
[4] A.H. Nayfeh, C.-M. Chin, J. Pratt, Perturbation methods in nonlinear dynamics—applications to machining dynamics, (1997).
[5] E. Budak, Y. Altintas, Analytical prediction of chatter stability in milling—part I: general formulation, (1998).
[6] B. Balachandran, M.X. Zhao, A mechanics based model for study of dynamics of milling operations, Meccanica, 35 (2000) 89-109.
[7] J.R. Pratt, A.H. Nayfeh, Chatter control and stability analysis of a cantilever boring bar under regenerative cutting conditions, Philosophical Transactions of the Royal Society of London. Series A: Mathematical, Physical and Engineering Sciences, 359 (2001) 759-792.
[8] N. Deshpande, M.S. Fofana, Nonlinear regenerative chatter in turning, Robotics and Computer-Integrated Manufacturing, 17 (2001) 107-112.

[9] F.C. Moon, T. Kalmar-Nagy, Nonlinear models for complex dynamics in cutting materials, Philosophical Transactions of the Royal Society of London. Series A: Mathematical, Physical and Engineering Sciences, 359 (2001) 695-711.
[10] B. Balachandran, Nonlinear dynamics of milling processes, Philosophical Transactions of the Royal Society of London. Series A: Mathematical, Physical and Engineering Sciences, 359 (2001) 793-819.
[11] M.S. Fofana, Delay dynamical systems and applications to nonlinear machine-tool chatter, Chaos, Solitons & Fractals, 17 (2003) 731-747.
[12] B.P. Mann, N.K. Garg, K.A. Young, A.M. Helvey, Milling bifurcations from structural asymmetry and nonlinear regeneration, Nonlinear Dynamics, 42 (2005) 319-337.
[13] E. Budak, E. Ozlu, Analytical modeling of chatter stability in turning and boring operations: a multi-dimensional approach, CIRP annals, 56 (2007) 401-404.
[14] E. Ozlu, E. Budak, Comparison of one-dimensional and multi-dimensional models in stability analysis of turning operations, International Journal of Machine Tools and Manufacture, 47 (2007) 1875-1883.
[15] L. Vela-Martínez, J.C. Jáuregui-Correa, O.M. González-Brambila, G. Herrera-Ruiz, A. Lozano-Guzmán, Instability conditions due to structural nonlinearities in regenerative chatter, Nonlinear Dynamics, 56 (2009) 415-427.
[16] H. Moradi, M.R. Movahhedy, G. Vossoughi, Dynamics of regenerative chatter and internal resonance in milling process with structural and cutting force nonlinearities, Journal of Sound and Vibration, 331 (2012) 3844-3865.
[17] H. Moradi, G. Vossoughi, M.R. Movahhedy, M.T. Ahmadian, Forced vibration analysis of the milling process with structural nonlinearity, internal resonance, tool wear and process damping effects, International Journal of Non-Linear Mechanics, 54 (2013) 22-34.
[18] M. Li, G. Zhang, Y.u. Huang, Complete discretization scheme for milling stability prediction, Nonlinear Dynamics, 71 (2013) 187-199.
[19] G. Jin, Q. Zhang, S. Hao, Q. Xie, Stability prediction of milling process with variable pitch cutter, Mathematical problems in engineering, 2013 (2013).
[20] C.-L. Liao, J.-S. Tsai, Dynamic response analysis in end milling using pre-twisted beam finite elements, Journal of materials processing technology, 40 (1994) 407-432.
[21] M. Salahshoor, H. Ahmadian, Continuous model for analytical prediction of chatter in milling, International Journal of Machine Tools and Manufacture, 49 (2009) 1136-1143.
[22] G. Catania, N. Mancinelli, Theoretical–experimental modeling of milling machines for the prediction of chatter vibration, International Journal of Machine Tools and Manufacture, 51 (2011) 339-348.
[23] M.R. Movahhedy, P. Mosaddegh, Prediction of chatter in high speed milling including gyroscopic effects, International Journal of Machine Tools and Manufacture, 46 (2006) 996-1001.
[24] S.A. Tajalli, M.R. Movahhedy, J. Akbari, Size dependent vibrations of micro-end mill incorporating strain gradient elasticity theory, Journal of Sound and Vibration, 332 (2013) 3922-3944.
[25] S.A. Tajalli, M.R. Movahhedy, J. Akbari, Chatter instability analysis of spinning micro-end mill with process damping effect via semi-discretization approach, Acta Mechanica, 225 (2014) 715-734.
[26] H. Tavari, M.M. Jalili, M.R. Movahhedy, Nonlinear analysis of chatter in turning process using dimensionless groups, Journal of the Brazilian Society of Mechanical Sciences and Engineering, 37 (2015) 1151-1162.
[27] M.M. Jalili, H. Emami, Analytical solution for nonlinear oscillation of workpiece in turning process, Proceedings of the Institution of Mechanical Engineers, Part C: Journal of Mechanical Engineering Science, 231 (2017) 3479-3492.
[28] M.M. Jalili, J. Hesabi, M.M. Abootorabi, Simulation of forced vibration in milling process considering gyroscopic moment and rotary inertia, Int J Adv Manuf Technol, 89 (2017) 2821-2836.
[29] A. Mokhtari, A. Mazidi, M.M. Jalili, Investigation of rotary inertial dynamic effects on chatter boundary in milling process using three-dimensional Timoshenko tool model, Proceedings of the Institution of Mechanical Engineers, Part K: Journal of Multi-body Dynamics, 233 (2019) 93-110.
[30] A. Mokhtari, M.M. Jalili, A. Mazidi, M.M. Abootorabi, Size dependent vibration analysis of micro-milling operations with process damping and structural nonlinearities, European Journal of Mechanics-A/Solids, 76 (2019) 57-69.
[31] A.H. Nayfeh, D.T. Mook, Nonlinear Oscillations, Wiley, New York, 1979, LD Landau and E. M. Lifshitz, Mechanics (Pergamon, New Y'ork, 1976), 338-348.
[32] H. Moradi, G. Vossoughi, M.R. Movahhedy, Experimental dynamic modelling of peripheral milling with process damping, structural and cutting force nonlinearities, Journal of Sound and Vibration, 332 (2013) 4709-4731.

[33] Z. Zhang, H. Li, G. Meng, S. Ren, Milling chatter suppression in viscous fluid: a feasibility study, International Journal of Machine Tools and Manufacture, 120 (2017) 20-26.
[34] X. Huang, X. Zhang, H. Mou, X. Zhang, H. Ding, The influence of cryogenic cooling on milling stability, Journal of Materials Processing Technology, 214 (2014) 3169-3178.